



European Coordination for Accelerator Research and Development

PUBLICATION

A sensitivity analysis for the stabilization of the CLIC main beam quadrupoles

Janssens, S (CERN) *et al*

06 October 2010

The research leading to these results has received funding from the European Commission under the FP7 Research Infrastructures project EuCARD, grant agreement no. 227579.

This work is part of EuCARD Work Package 9: **Technology for normal conducting higher energy linear accelerators.**

The electronic version of this EuCARD Publication is available via the EuCARD web site <<http://cern.ch/eucard>> or on the CERN Document Server at the following URL : <<http://cdsweb.cern.ch/record/1297980>>

A sensitivity analysis for the stabilization of the CLIC main beam quadrupoles

S. Janssens¹, C. Collette¹, K. Artoos¹, P. Fernandez Carmona¹, C. Hauviller¹

¹ Engineering Department, European Organization for Nuclear Research (CERN), Geneva 23, 1211 Geneva, Switzerland

e-mail: Stef.Marten.Johan.Janssens@cern.ch

Abstract

In particle colliders (like the LHC), particles are highly accelerated in a circular beam pipe before the collision. However, due to the curved trajectory of the particles, they are also losing energy because of the so-called Bremsstrahlung. In order to bypass this fundamental limitation imposed by circular beams, the next generation of particle colliders will accelerate two straight beams of particles before the collision. One of them, the Compact Linear Collider, is currently under study at CERN. The machine is constituted of a huge number of accelerating structures (used to accelerate the particles) and quadrupoles (electromagnets used to focus the particles). The latter ones are required to be stable at the nanometer level. This extreme stability has to be guaranteed by active vibration isolation from all types of disturbances like ground vibrations, ventilation, cooling system, or acoustic noise. Because of the huge number of quadrupoles (about 4000), it is critical that the strategy adopted for the active isolation is robust to any type of uncertainty: variations of the mechanical properties of the structure, variations of the level of the above mentioned disturbance sources, variations of the properties of the actuators and sensors, variations of the temperature, etc. In this paper, two active isolation strategies are investigated: one using soft supports and one using hard supports. These strategies are compared; their advantages and performances are discussed. Then, in order to quantify their robustness, a systematic sensitivity analysis against the different types of uncertainty is performed.

1 Introduction

The future Compact Linear particle Collider (CLIC) under study at CERN will require the reduction of vibrations in heavy electromagnets also called quadrupoles. Any oscillation of one quadrupole deflects the beam, and reduces the luminosity, a measure of collision quality. More precisely, it has been estimated that the integrated Root Mean Square (RMS) of the displacement, defined as

$$\sigma_x(f) = \sqrt{\int_f^\infty \Phi_x(\nu) d\nu} \quad (1)$$

with Φ_x the power spectral density of the quadrupole motion, must stay below 1 nm [2] for $f = 1$ Hz to ensure sufficient performances as shown in Figure 1a.

Additionally, about 80 quadrupoles should have the capability to move by steps of ten nanometers every 20 ms [3], with a precision of ± 1 nm shown in Fig. 1b.

The paper is organized as follows. In the second section of this paper, models of different isolation systems are developed. Two strategies are investigated, one using a soft and one using a hard support. In the third sec-

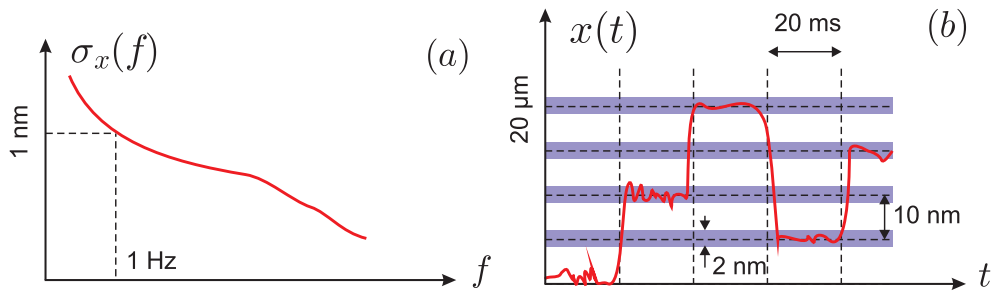


Figure 1: The integrated RMS requirement a) and the positioning requirements b) for CLIC.

tion a comparison is made between the models by comparing the sensitivity to sensor noise and disturbance forces. Finally a conclusion is drawn.

2 The models

Two main strategies can be applied to perform vibration isolation. A soft strategy which reduces the transfer function T_{wx} , between the quadrupole vibration x and the ground vibration w , around the natural frequency. The second strategy is the hard mount strategy which reduces the vibrations in front of the natural frequency of the system. Changing the stiffness lowers the natural frequency of the system as can be seen in Fig. 2a. This has also an effect on the ability of the system to cope with disturbance forces. The softer the system, the bigger the displacement that is caused by the disturbance force. This is shown in Fig. 2b by changing the stiffness and looking at the transfer function between the payload mass position x and the disturbance force F_d also called the compliance. The higher the compliance the more the payload mass is influenced by the disturbance force.

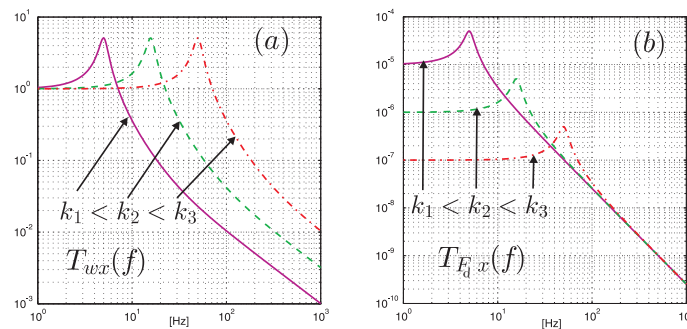


Figure 2: The effect of the stiffness on the transfer function between the ground w and the mass x a) and the transfer function between the disturbance force F_d and the mass position x b).

This effect is studied on several models based on already existing strategies. First the models are presented and then a comparison is made in section 3.

2.1 Soft Strategy

An example of a soft strategy solution is shown in Fig. 3. This strategy is described in [11], [12] and [5]. It reduces the high natural frequency of the the piezo actuator which has a stiffness of $k_a = 480e6$ N/m. An elastomer is used between an intermediate mass and the quadrupole in order to bring the natural frequency down to 10 Hz. A capacitive sensor is used to measure the relative distance between the quadrupole and the intermediate mass.

The equation of motion for the quadrupole is

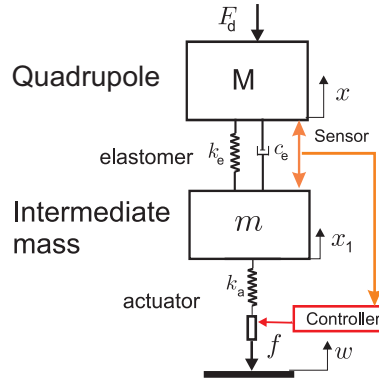


Figure 3: The Soft Strategy with a capacitive sensor.

$$M\ddot{x} + c_e(\dot{x} - \dot{x}_1) + k_e(x - x_1) = F_d \tag{2}$$

and for the intermediate mass

$$m\ddot{x}_1 + c_e(\dot{x}_1 - \dot{x}) + k_e(x_1 - x) + k_a(x_1 - w) = f \tag{3}$$

with $f = -H(s)(x - x_1)$ in which $H(s)$ is a combination of a first order high pass filter at 0.7 Hz to remove any low frequency drift, a first order low pass anti-aliasing filter at 50Hz and a lag at 30 Hz to increase stability.

Equation 2 results in a transfer function between the position of the quadrupole x and the position of the intermediate mass x_1 in the Laplace domain, equal to

$$G_2 = \frac{X(s)}{X_1(s)} = \frac{c_e s + k_e}{Ms^2 + c_e s + k_e} \tag{4}$$

Equation 3 is rewritten in the Laplace domain and transfer function G_2 is used to transform $X_1(s)$ in $X(s)$ so the equation can be written as a function of the quadrupole position $X(s)$

$$[ms^2 + c_e s + k_e + k_a]X_1(s) = k_a W(s) - H(s)(X(s) - X_1(s)) + (c_e s + k_e)X(s) \tag{5}$$

$$[ms^2 + c_e s + k_e + k_a]X(s) = G_2[k_a W(s) - H(s)(1 - 1/G_2)X(s) + (c_e s + k_e)X(s)] \tag{6}$$

$$X(s) = G[G_2 k_a W(s) - H(s)KX(s)] \tag{7}$$

with $G = \frac{1}{ms^2 + (c_e s + k_e)(1 - G_2) + k_a}$ and $K = G_2 - 1$. The block diagram of the system is shown in Fig. 4.

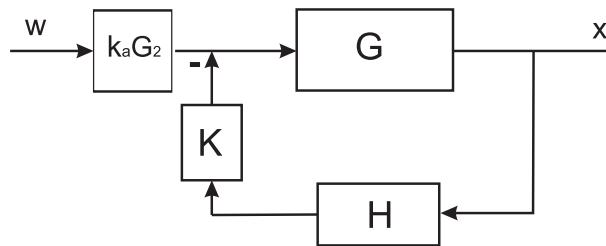


Figure 4: The block diagram for the Soft Strategy with a capacitive sensor.

The stability margins can be calculated with the help of the open-loop gain. The point at which a system becomes unstable is located at the point of neutral stability. This point can be calculated for both the gain and the phase with the help of the characteristic equation $1 + G(s)H(s)K(s) = 0$ [9].

$$|G(s)H(s)K(s)| = 1 \tag{8}$$

$$\phi(G(s)H(s)K(s)) = -\pi \tag{9}$$

The system is stable if the algebraic value of the phase ϕ is larger than $-\pi$ and smaller than π for all frequencies where the amplitude $|K(s)G(s)H(s)|$ is larger than 1 [9].

A lag compensator can be used to reduce the gain at high frequency without affecting the gain at low frequency. This allows for the reduction in the cross over frequency and increases the phase margin. The open-loop transfer function is shown in Fig.5.

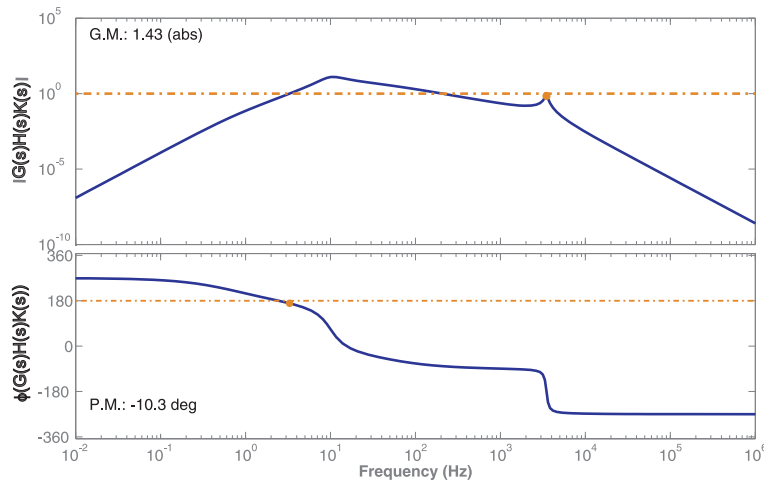


Figure 5: The open-loop transfer function of the Soft Strategy.

The Soft Strategy has a phase margin of 10 degrees and a gain margin of 1.43 which is well inside the stability margins. The resulting closed-loop transfer function is studied further in section 3.

2.2 Hard mount

Two main configurations are considered for a hard mount vibration isolation system. The first system is based on [15],[13] and [14], shown in Fig. 6a, with the reference mass situated on the ground measuring its position in relation to the ground motion w . The second configuration is based on [10],[8] and [5], where the position of the reference mass x_1 is measured in relation with the quadrupole position x , shown in Fig. 6b.

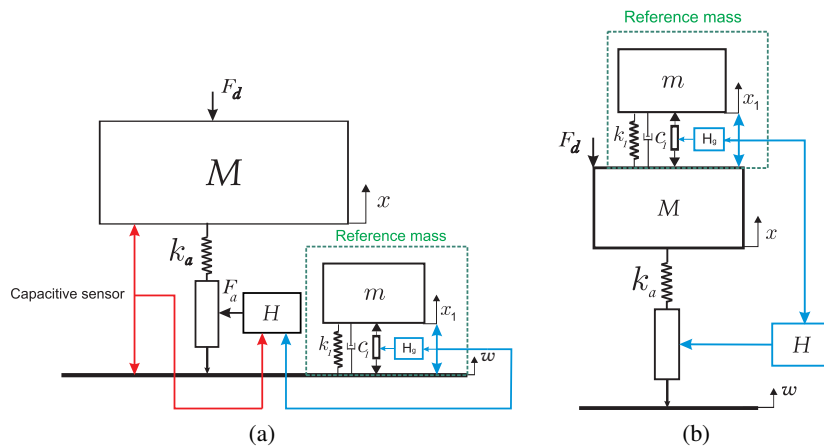


Figure 6: The hard mount 1 (a) and hard mount 2 (b) test configurations.

The reference mass $m = 0.01$ kg is suspended in a way that it has a natural frequency of 1.6 Hz and a damping ratio of $\xi = 0.017$ [6].

It uses an acceleration and velocity feedback to reduce its natural frequency and damp the peak at the natural frequency. The driving forces can be calculated from

$$F_{con,fig1} = -mG_gW(s)s^2 - 2m\omega_0H_gW(s)s \tag{10}$$

$$F_{con,fig2} = -mG_gX(s)s^2 - 2m\omega_0H_gX(s)s \tag{11}$$

with $G_g = 2300$ and $H_g = 46$ and $\omega_0 = \sqrt{\frac{k_1}{m}}$ as specified in [6]. The closed-loop transfer function for the reference mass for Hard mount 1 is given by

$$G_2 = \frac{X_1(s)}{W(s)} = \frac{c_1s + k_1}{ms^2(1 + G_g) + s(c_1 + 2m\omega_0H_g) + k_1} \tag{12}$$

This is the same for Hard mount 2 with the change of $W(s)$ being replaced by $X(s)$. The position of the reference mass is measured with a capacitive gauge.

2.2.1 Hard mount 1

Hard mount 1 uses a capacitive sensor to measure the relative position between the quadrupole x and the ground w . Together with the position measurement of the reference mass, these two are combined to calculate the actuator force

$$F_a = -H(s)(X(s) - X_1(s)) \tag{13}$$

with

$$H(s) = g_p + g_v s \tag{14}$$

The equation of motion for the quadrupole in the Hard mount 1 configuration is

$$X(s) = G[k_aW(s) - H(s)(X(s) - X_1(s))] \tag{15}$$

$$= G[k_aW(s) - H(s)(X(s) - W(s)G_2)] \tag{16}$$

with G

$$G = \frac{1}{Ms^2 + k_a} \tag{17}$$

The block diagram of Hard mount 1 is shown in Fig. 7.

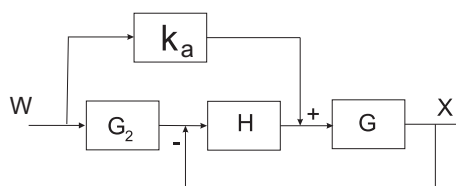


Figure 7: The block diagram of Hard mount 1 strategy.

To H a first order high pass filter at 0.7 is added to exclude the drift. A first order low pass filter at 50 Hz functions as an anti aliasing filter and a Lead is added to increase the stability by increasing the phase margin. The capacitive gauge dynamics can also be added in H . The transfer function of the capacitive sensor for the reference mass is considered constant. Therefore no additional poles are added to the control loop.

2.2.2 Hard mount 2

Hard mount 2 only uses the measurement provided by the capacitive sensor of the reference mass. The actuation force for Hard mount 2 is given by

$$F_a = -H(s)(X_1(s) - X(s)) \quad (18)$$

with

$$H(s) = g_p + g_v s \quad (19)$$

$H(s)$ again a signal conditioning transfer function and a constant transfer function for the capacitive sensor. The equation of motion for the quadrupole becomes

$$X(s) = G[k_a W(s) - H(s)(G_2 - 1)X(s)] \quad (20)$$

with

$$G = \frac{1}{Ms^2 + (c_1 s + k_1)(1 - G_2) + k_a} \quad (21)$$

The block diagram of Configuration 2 is shown in Fig. 8. In H the same low pass filter, high pass filter and Lead is included.

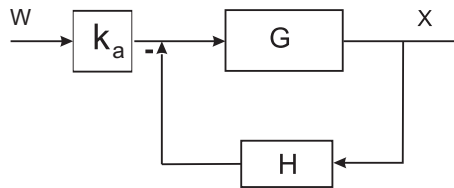


Figure 8: The block diagram of the Hard mount 2 strategy.

2.2.3 Stability study

The open-loop graph for both configurations is shown in Fig. 9. In order to study the effect of the high stiffness on the stability margins, Hard mount 1 has been recalculated by changing the stiffness k_a to a lower value resulting in a natural frequency of 2 Hz which will be called Hard mount 3.

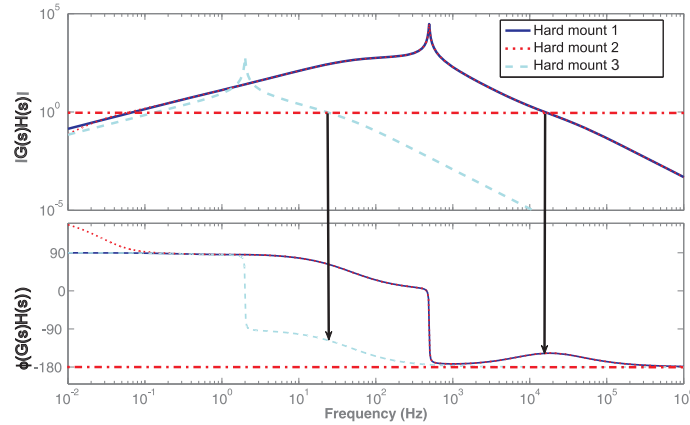


Figure 9: Open-loop transfer functions.

The two hard mount configurations are very similar and both have nearly the same stability margins. When including the lead the phase margin is 30 degrees. When the gains g_v and g_p remain the same but the natural frequency of the actuator is greatly reduced in Hard mount 3, the phase margin increases and no lead is necessary. Using a hard mount decreases stability margins but this can be resolved by using a lead near the crossover frequency. The closed-loop transfer function is given in section 3.

3 Soft vs Hard

As can be seen in Fig. 10 the closed-loop transfer function for the Soft Strategy only starts reducing vibrations from 10 Hz. This is only a very basic representation of the Soft Strategy and using different sensors could improve the performance. The Soft version of Configuration 1 surpasses the transfer function of the hard configurations at around 100 Hz. The Hard mount 3 isolates the quadrupole much more at high frequencies.

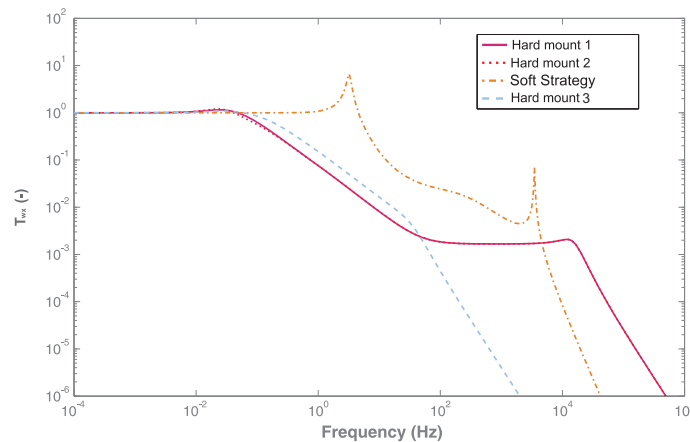


Figure 10: Closed-loop transfer functions.

The tracking capabilities, the disturbance force rejection and sensor noise influence can be studied through the sensitivity S and complementary sensitivity T curves of the different systems. The sensitivity for the soft strategy is given by

$$S = \frac{1}{1 + GHK} \tag{22}$$

and for the Hard mount strategies the sensitivity is given by

$$S = \frac{1}{1 + GH} \quad (23)$$

The complementary Sensitivity for both the soft strategy and the Hard mounts is found from

$$T = 1 - S \quad (24)$$

In order to have good tracking capabilities and disturbance force rejection S should be small and T should be large. In order to have less influence of noise however, S should be large and T should be small [4]. This shows the classical trade-off in feedback control. The sensitivity curves calculated from eq. 22 for the Soft Strategy and eq. 23 for Hard mount 1, 2 and 3 are shown in Fig. 11. The complementary sensitivity curves, calculated from eq. 24 are shown in Fig. 12.

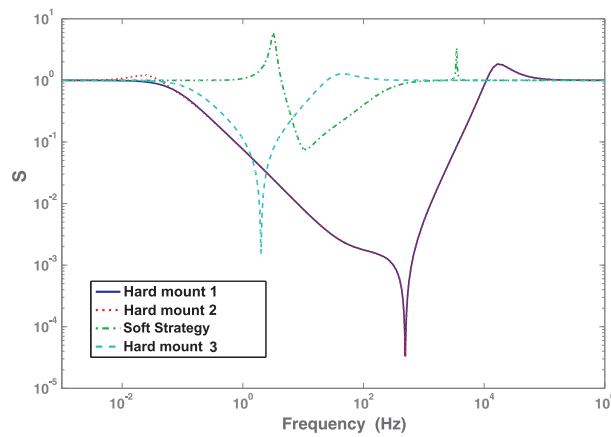


Figure 11: Sensitivity curves.

Figure 11 and Figure 12 show that Hard mount 1 and 2 are very good in tracking and disturbance force rejection in a very large bandwidth. When the stiffness of the actuator for Hard mount 1 is reduced as it has been done for Hard mount 3, the bandwidth in which the influence of disturbance forces is small, is greatly reduced. Also the tracking performance is greatly reduced making it less suitable for positioning. The same can be seen for the Soft Strategy.

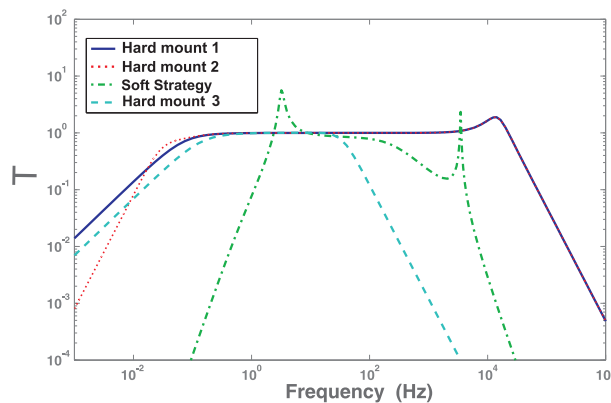


Figure 12: Complementary Sensitivity curves.

The fact that S is small and T is large in a large bandwidth for Hard mounts 1 and 2 also means that it is more susceptible to sensor noise. To study this effect, error budgeting is performed as was done in [7]. This is done by adding a noise function of a sensor to the feedback signal just in front of H in the block diagram

for Hard mount 1 and Hard mount 3 shown in Fig. 7. This simulates the sensor noise. A simulation is run without ground vibration input $w = 0$ but with the noise input. The resulting square root of the Power Spectral Density for the original noise function, the propagated noise function at the quadrupole position x for both Hard mount 1 and Hard mount 3 is shown in Fig. 13.

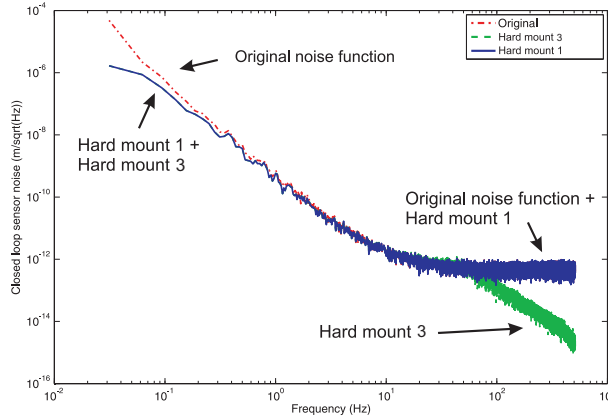


Figure 13: Noise propagation in Configuration 1 and Configuration 1 Soft.

Comparing Fig. 12 with Fig. 13 shows the connection between the complementary sensitivity and the noise. Before 0.1 Hz the noise is slightly reduced for both soft and hard configuration. After 100 Hz, the noise for the soft system is reduced significantly while the hard configuration continues to follow the original noise function making it more susceptible to noise at high frequency.

An overview of all the found properties for the different configurations is shown in Table 1.

	Hard mount 1	Hard mount 2	Soft Strategy	Hard mount 3
Vibration isolation	++	++	+	++
Stability	+	+	+	++
Disturbance force rejection	++	++	--	-
Positioning (Tracking)	++	++	--	--
Noise Sensitivity High freq.	--	--	++	++
Noise Sensitivity Low freq.	+	+	++	+

Table 1: Properties overview.

4 Conclusion

In this paper it was found that both Soft and Hard mount strategies are capable of performing vibration isolation. The hard mounts 1 and 2 are superior in handling disturbance forces and positioning but are more susceptible to high frequency noise than the soft strategies. This paper shows the importance of performing sensitivity analysis and error budgeting in order to get a complete image of a systems performance. Future work will consider a flexible payload, as the quadrupole has its own eigenmodes and a flexible support as the quadrupole will be positioned on an alignment stage in order to study the effect on the controller.

References

- [1] C. Collette, K. Artoos, A. Kuzmin, S. Janssens, M. Sylte, M. Guinchard, C. Hauviller, *Active quadrupole stabilization for future linear particle colliders*, Nuclear Instruments and Methods in Physics Research A, Elsevier (2010).
- [2] CLIC, *Clic stabilization website*, <http://clic-stability.web.cern.ch/clic-stability/>.
- [3] Schulte, D, *Beam based alignment in the new clic main linac*, Particle Accelerator Conference (2009).
- [4] G.F. Franklin, J.D. Powell, and A. Emami-Naeini. *Feedback Control of Dynamic systems (3rd edition)*, Addison-Wesley Publishing Company Inc., Reading, Massachusetts (1994).
- [5] A.A. Hanieh. *Active Isolation and Damping of Vibrations via Stewart Platform*, PhD thesis, Université Libre de Bruxelles, Active Structures Laboratory (2003).
- [6] J.M. Hensley, A. Peters, and S. Chu. *Active low frequency vertical vibration isolation*, Review of Scientific Instruments (1999), vol. 70, No. 6, pp. 2735-2741.
- [7] K. Kar-Leung Miu. *A Low cost, DC-Coupled Active Vibration System*, PhD thesis, Massachusetts Institute of Technology (2008).
- [8] P.G. Nelson. *An active vibration isolation system for inertial reference and precision measurement*, Review of Scientific Instruments (1991), vol. 62, No. 9, pp. 2069-2075.
- [9] A. Preumont. *Vibration Control of Active Structures An Introduction (2nd edition)*, Kluwer Academic Publishers, Dordrecht (2002).
- [10] P.R. Saulson. *Vibration isolation for broadband gravitational wave antennas*, Review of Scientific Instruments (1984), vol. 55, No. 8, pp.1315-1320.
- [11] D.W. Schubert, A.M. Beard, S.F. Shedd, M.R. Earles Jr., and A.H. Von Flotow. *Stiff actuator active vibration isolation system*, Technical Report Patent Number: 5,823,307, United States Patent (1997).
- [12] D.W. Schubert, A.M. Beard, and A.H. von Flotow. *A practical product implementation of an active/passive vibration isolation*, SPIE (1994), vol. 2264.
- [13] M.J. Vervoordeldonk, T.A.M. Ruijl, and R.M.G. Rijs. *Development of a novel active isolation concept*, ASPE Spring Topical Meeting (2004).
- [14] M.J. Vervoordeldonk, T.A.M. Ruijl, R.M.G. Rijs, and J.C.A. Muller. *Actuator arrangement for active vibration isolation comprising an inertial reference mass*, Technical Report Patent Number: US 2007/0035074 A1, United States Patent (2007).
- [15] M.J. Vervoordeldonk and H. Stoutjesdijk. *Recent developments, a novel active isolation concept* 6th euspen International Conference (2006), Baden bei Wien.